J. Agric. Sci. Technol. (2009) Vol. 11: 67-80

Evaluation of the Capability of Landsat MSS Data for Mapping Landforms in Arid Regions: A Case Study in the Centre of Iran

M. Naderi Khorasgani[1*], and M. De Dapper[2]

ABSTRACT

This research was performed to evaluate the potentials of Landsat MSS data for mapping land features in arid zones of southeastern Esfahan, Iran. Databases of the area were formed using all available relevant maps and reports which were supported by fieldwork. A supervised image classification approach was used and thirty-two training areas were applied. Separability of the spectral classes was examined using feature space plots of imagery data and self-classification of training areas. The accuracy of the classification was examined by using test and random pixels. The results show the potential of Landsat data for the discrimination of landforms and zones of the playas. Sand deposits (deflated sands and Barchans) expressed different spectral reflectance which could be due to mineralogy of these features. Soil classes differing in moisture content and salinity located on the soil line and limestone classes located along the soil line. The applied imagery data disable to discriminate Barchans from Bare soil I and Andesitic fans from Grey limestone. After image classification the spectral classes were merged to form landforms. The main landforms were mountains, piedmonts, sand dunes, valleys and playas. The results indicate that integration of field observation and supervised classification can compensate for the lack of detailed topographic maps in some areas.

Keywords: Barchan, Landform, Landsat MSS, Piedmont, Playa, Soil line, Supervised classification.

INTRODUCTION

Surveying morphology and landforms has traditionally been conducted using aerial photos and photogrammetric techniques. Coventional photo-interpretation for landform extraction and geo-pedology was introduced by Zink (1988) and Zink and Valenzula (1990). Many researchers implemented quantitative landsacape analysis using digital terrain analysis and landform morphometry (Lane *et al*., 1998; Odeh *et al*., 1994; Schmidt *et al*., 1998). Burrough *et al*. (2000) used unsupervised fuzzy classification to detect landform facets. Using imagery data by extending the synoptic view provides more facilities for more accurate mapping and aids understanding of the landform and so is superior to aerial photos (Muller *et al*., 1993; Yates *et al*., 1993; Donoghue *et al*., 1994; Milton *et al*., 1995; McManus *et al*., 1999; Rainy *et al*., 2003). Hengle and Rossiter (2003) extracted nine limited terrain parameters from digital elevation model. They used the terrain parameters, supervised classification approach and maximum likelihood classifier techniques to classify aerial photos. They reported that the accuracies for classification of hill land, plain and entire area were 58.2, 39.1 and 45.3 percent, respectively. They concluded

[1] Department of Soil Science, Faculty of Agriculture, Shahrekord University, P. O. Box: 115, Shahrekord, Islamic Republic of Iran.

[*] Corresponding author, e-mail: naderi@agr.sku.ac.ir

[2] Gent University, Earth Sciences Institute, Krijaslaan, 281/S8, B. 9000, Ghent, Belgium.

[DOR: 20.1001.1.16807073.2009.11.1.2.1]

that fine detail of landscapes had not been achieved through aerial photos. Leblance *et al*. (2006) used Landsat TM, Landsat MSS and MODIS imagery data for detecting paleoshorelines of Megalake Chad in Africa. They reported that the aforementioned remote sensing data provided new information by enabling large landforms to be examined fully and in context with the surrounding environment.

The overall aim of this study was to examine the feasibility of using digital Landsat MSS data accompanied by fieldwork to detect landforms of an arid region in the centre of Iran. Use of remote sensing data and a digital elevation model and its derivates provide a lot of information for landform analysis. In the absence of large scale topographic maps, aerial photos are another alternative but very time-consuming. The visible and infrared bands of satellite data do not provide any information about topography of a landscape but spectral sensitivity of such data should not be ignored. Erosion, weathering, groundwater table, climate, biological activities, topography, slope, time and aspect impact the landscape materials and especially soil surface spectral responses. The spectral reflectance of landforms is the result of such interactions and could be captured by remote sensing sensors for landform classification.

MATERIALS AND METHODS

Study Area

The study area is situated between 31° 45' to 32° 34' N and 51° 50' to 52° 53' E. It covers an area about 34,200 km^2 in the centre of Iran (figure 1). The Zayanderood River (a source of freshwater in this arid land) crosses the north of the area and pours into Gavkhoni playa in the East. The major physiographic units of the study area are mountains, piedmonts, sand dunes, alluvial plains and the playa. The highest altitude of the area is 2,100 m above sea level and the lowest point is Gavkhoni playa with an altitude of 1,300 m above sea level. According to the De Martonne index (Alizadeh 1990) and the climatological data of Varzane station, the climate of the area is arid. The maximum and minimum temperatures are 37°C and 5.6°C and occur in July and December, respectively. According to Ganji (1955) the mean annual precipitation for the study area is less than 150 mm. Krinsley (1970) studied the Esfahan-Sirjan watershed and reported that Esfahan region is the moistest part of this watershed. The major factors which influence land degradation are topography, lithology and stratification of sediments. The saline fluvial materials from south and north of the study area and northwest of Esfahan charge the area with brackish water. Saline-gypsiferous marl deposits are exposed on the upper terraces in the Northwest and are buried in lower altitudes by fluvial materials. A thick and massive clayey horizon is developed close to the surface of alluvial plains which hinders the natural drainage of soils and aids development of marshes and salt crusts.

Database Construction

The soil map of 44,000 ha of the area (northern part) was prepared by the Soil Institute of Iran (1976) in which three landforms and 8 soil mapping units were discriminated. Cloud-free images of Landsat MSS data with four bands dated 27 May 1976 were provided by the Remote Sensing Centre of Iran. The images consist of 1,169 rows and 1,632 columns.

The database of the study area was formed using all relevant maps and reports. Topographic maps of the area (1: 50,000 scale) with a major isoline interval of 100 m and minor isoline interval of 20 m were used. The isoline intervals are too large to study the microtopography of alluvial plains. Available geological maps consists of: a) the geological map of Iran (National Iranian Oil Co., 1978) in scale of 1: 1,000,000 (in two sheets) and b) the Geological Map of the Esfahan Quadrangle in scale of 1: 250,000 (Zahedi, 1976) which only covers 30% of

[DOR: 20.1001.1.16807073.2009.11.1.2.1]

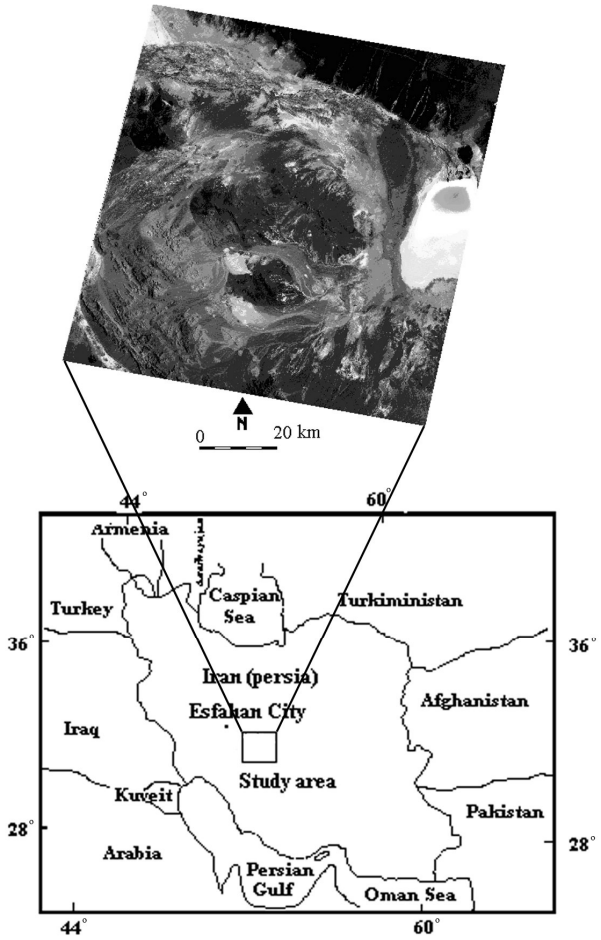

Figure 1: Location and standard false color composite of study area.

the area. Both of them were used for the determination of training areas.

Field Observations

An intensive fieldwork study was arranged and geomorphologic units of the area were studied in the field using attribute data such as false color composite (FCC) and topographic maps. To have a general idea of the geomorphologic units we visited the area along two routes or transects, in North-South and West-East directions. As the salinity of land covers impacts the soil reflection, the soil surface salinity of training areas also was determined using a portable Electrical Conductivity meter and the stratification of land covers was studied in the field by considering available data such as soil and geological maps and reports. The training areas were determined for supervised classification (Table 1) and some parts were used as test sites or ground truth for testing the accuracy of image classification. Both areas were addressed to the false color composite.

Image Classification Strategy

A supervised classification approach was used for remotely sensed data classification which depends on the statistical characteristics

[DOR: 20.1001.1.16807073.2009.11.1.2.1]

Table 1. Brief description of training areas.

Training Area	Description
1. Moderately salt affected vegetation I	Moderately saline soils, moderately dense vegetation based on NDVI and standard FCC, soil surface texture is clayey.
2. Moderately salt affected vegetation II	A moderately saline soil, sparse to moderately dense vegetation according to the NDVI, soil surface texture is clayey.
3. Moderately salt affected vegetation III	Moderately saline soils, silty clay loam, tolerant crops to salinity.
4. and 5. are Moderately salt affected vegetation IV and V respectively	Moderately salt affected vegetation, silty clay loam to silty loam, these two classes are spectrally different from each other due to the crops' moisture content.
6. Playas water zone	Water zone of the Gavekhoni playa, severely saline, brackish water in the centre of playa.
7. Saturation zone of playa	Transitional zone between water zone of the playa and the pore water zone, bare.
8. Pore water zone of playa	Pore water zone of playas, mostly whitish NaCl, mine of salt, water table shallow, mostly in the playas of Gavkhoni, bare.
9. Salt crust zone of playa	Dry, a dense and bare salt crust around the playa of Gavekhoni.
10. Limestone I	Grey limestone with orbitolinas and ammonites.
11. Limestone II	Marl bedded orbitolinas limestone with ammonites.
12. Limestone III	Grey limestone containing orbitolinas and ammonites.
13. Limestone IV	Marl thin bedded limestone containing inoceramus and cenomanian glauconite, sandy limestone, shale with abundant ammonites.
14. Limestone V	Brown limestone, with ammonites and orbitolinas.
15. Grey limestone and Andesitic fans	Composed of grey limestone with ammonites and orbitolinas and andesitic alluvial fans, a lot of boulders at the surface, all are bare and dry.
16. Salt crust I	Severe saline soils, with a developed salt crust at the surface, water table at 1.2-2 m, bare.
17. Salt crust II	Severe saline soils, with a dense salt crust, water table at 1.2-2 m, bare, with crystalline salts and gypsum through the profile.
18. Salt crust III	Severe saline soils, with a lot of crystalline salts through the profile, with a dense salt crust, bare.
19. Salt crust IV	Severe saline soils, with a lot of crystalline salts, with a developed network of rills and gullies and a thin and loose crust at the surface, well drained.
20. Fallow I	Moderately saline soils, dry, silty clay loam, soil surface bright.
21. Fallow II	Except the spectral signature all the characteristics are similar to Fallow I.
22. Fallow III	A low saline soil, in fallow condition, soil surface texture is silty clay loam.
23. Low salt affected vegetation I	Non to low saline soils, relatively dense vegetation according to the NDVI, silty clay loam texture at the surface.
24. Low salt affected Vegetation II	Non to low saline soils, silty clay loam, and relatively dense vegetation based on NDVI and standard FCC.
25. Low salt affected vegetation III	Low saline soils, silty clay loam, moderately dense vegetation based on NDVI and standard FCC.
26. Bare soil I and Barchans	Moderately saline soils, silty clay texture, covered with heterogeneous boulder and gravel of limestone, quartz and desert varnish. The spectral signature of stable sand dunes or Barchans (which are located in the west of the Gavkhoni playa) and Bare soil I are identical.
27. Bare soils II	Moderately saline soils, bare, the same as bare soils I but without desert varnish cover, some erosion evidences at the surface, soils are exposed.
28. Gypsiferous plateau	Gypsiferous plateaus, with gravel at the surface, due to the erosion of soil surface the gypsum pendants are exposed.
29. Deflated sands	Very active sands, moving in the direction of the dominant wind of the area (from the west to the east), bare, covered old river terraces and pediments.
30. Basaltic Mountain	The volcanic mountain, basaltic materials, dark, bare, with debris flow materials, some wind deposits in the foot slope.
31. Waterlogged areas	Severely saline, some parts severely alkali, in some parts with a thin layer of water at the surface and some vegetation, in some parts with a high organic matter at the surface.
32. River (irrigation canals and flooded areas)	Deep and shallow water of the river and flooded areas, mixed pixels of water and vegetation in the river and in the both sides of the river and the irrigation canals.

[DOR: 20.1001.1.16807073.2009.11.1.2.1]

of land covers and the training areas provide such information. According to Richards (1986) for N dimensional multispectral space at least N+1 samples (pixels) are required to avoid covariance matrix being singular. Swain and Davis (1978) recommended as a practical minimum that 10 N samples per spectral class be obtained for training, with 100 N being highly desirable if it can be attained. By considering all the suggestions mentioned (Mather, 1999; Webster and Oliver, 1990; Lillesand *et al*., 2004) and the aerial extension of land covers we introduced between 40 and 936 training pixels to the classifier for each spectral class and, totally, 6,320 pixels were introduced to the classifier. We selected several training areas for each spectral class throughout the area to avoid biased sampling and to consider all the within class variations. A random single-sampling strategy was used for selecting pixels from training areas. The ILWIS GIS software (2001) was used for digital image processing. All four bands were applied for image classification. The Gaussian maximum likelihood classifier was used and the separability of spectral classes were examined by comparing the means and standard deviations of training areas, checking the clusters of the training areas in the feature space plot of pair bands and self-classification of the training areas.

Where the spectral classes overlapped in all approaches we merged them and other methods were used for discrimination of them. The accuracy of classification was determined using test and random pixels as the ground truth in a confusion matrix (Table 4). The classified images were corrected for geometric distortions using GPS and topographic maps. About 50 ground control points were selected and finally, 16 well distributed points were applied for geometric correction. The second order bilinear function was applied for georefrencing. The root mean square error (RMSE) of the function was 0.48. The nearest neighbor interpolation approach was used and the map was resampled.

RESULTS AND DISCUSSION

Data Processing

Table 2 shows the standard deviations, means and the range of histograms of imagery data. Standard deviations of the first three bands are very close to one another and the digital value of land covers are distributed over the brightness range.

Chavez *et al*. (1982, 1984) introduced the optimum index factor (OIF) for selecting the

Table 2. The statistical characteristics of four MSS bands.

Band	Minimum	Maximum	Mean	St. Deviation[a]
MSS4	0	127	54.25	19.41
MSS5	0	127	80.24	19.57
MSS6	0	127	82.82	19.07
MSS7	0	63	32.00	7.90

[a] Denotes standard deviation.

Table 3. The optimum index factor values for MSS imagery data.

Rank	Bands	OIF Value
1	123[a]	23.37
2	124[b]	21.52
3	134	21.21
4	234	18.11

[a] The numbers of 1, 2, 3 and 4 denote MSS band of 4, 5, 6 and 7, respectively.
[b] Refers to the standard false color composite.

[DOR: 20.1001.1.16807073.2009.11.1.2.1]

most informative bands for display and classification. Greenbaum (1987) explained that summation of standard deviation and intercorrelation coefficients of bands could be used for OIF calculation:

$OIF = \sum(\text{Standard deviation}) / \sum|\text{Correlation coefficient}|$

Table 3 shows the OIF values for all three possible combination bands. The table indicates that the standard FCC is located in the second rank.

Spectral Signature of Training Areas

As Table 1 indicates for an informational class, for instance salt crust, there are several spectral classes due to differences in moisture content, organic matter content and/or chemical characteristics. In this table, cultivated areas (like salt affected vegetation) are expressed in eight, fallow lands in three, limestone in five, bare soils in two, playa in four and salt crusted areas in four spectral classes.

By plotting radiance measured in the visible red band against radiance in the near infrared for an area, bare soil pixels will lay along a hypothetical line which is called the soil line (Mather, 1999). Figure 2 illustrates the feature space plot of bands MSS5 and MSS7. The geomorphologic units of the playa are located in the right side of the space. The clusters of water zone, saturation zone and pore water zone of playa express a low, medium and high reflection on MSS7 band, respectively. The clusters of severe and moderate saline soils (classes 16, 17, 18, 19 and 21) are located in the upper parts of the feature space and express a relatively high reflection in both bands MSS5 and MSS7. Likewise, Everitt *et al*. (1988) measured the reflection spectra of saline and non saline soils in the field and expressed that the reflection of saline soils is higher than of the non saline soils in all parts of the visible and near infrared regions of the spectrum.

The salt crust zone of playa is located in the upper part, close to and below the soil line. The clusters of waterlogged areas and bare soils are located in the lower part while fallow lands with dry surfaces are located in the upper part of the soil line; such findings have been reported by other researchers also (Richadson and Wiegand, 1977; Baumgardener *et al*., 1985; Mather, 1987; Rencz, 1999). The pixels of salt crusted areas are located on the soil line and the reflection of salt crust IV is very high due to the efflorescence of sodium chloride salts at the surface. The Andesitic and Basaltic rocks (accompanied by Grey limestone) occupied an area in the lowest part of the soil line. Different kinds of limestone are located above and along the soil line and formed a line which could be named the limestone line. The MSS bands of 4, 5 and 6 are rescaled from 0-63 to 0-127 (Lillesand *et al*., 2004). MSS7 is the only band that shows the spectral reflection of playas precisely. Shaw and Thomas (1977) explained that playas generally consists of three zones: 1) saturated zone, 2) pore water zone and 3) salt crust zone. As the Zayanderood River pours into the playa even in the summer the centre of Gavekhoni playa is covered with brackish water which is called the water zone of playa (Figures 1 and 2). In the feature space plot of MSS5 and MSS7 the water zone of the playa has the lowest reflection on MSS7 band. This land cover was indicated as a columnar cluster in this plot. There is a transitional zone between the water zone and the pore water zone which is known as the saturation zone of the playa. The cluster of the saturation zone of the playa is between the pore water zone and the water zone in the feature space plot of MSS5-MSS7 (Figure 2).

The pore water zone of the playa has the highest reflection in all bands except green. Likewise, Chinese researchers reported that solonchaks express the highest reflection between 0.6 and 0.7 micron (Academia Sinica Institute of China, 1987). The standard deviation of this class on MSS5 is zero (Figure 2). The pore water zone is surrounded by the salt crust zone. The spectral signatures of these four zones are shown in Figure 3.

Ekbal *et al*. (1995, unpublished data) studied two North-South transects in the Gavkhoni playa. They analyzed the saline water of

[DOR: 20.1001.1.16807073.2009.11.1.2.1]

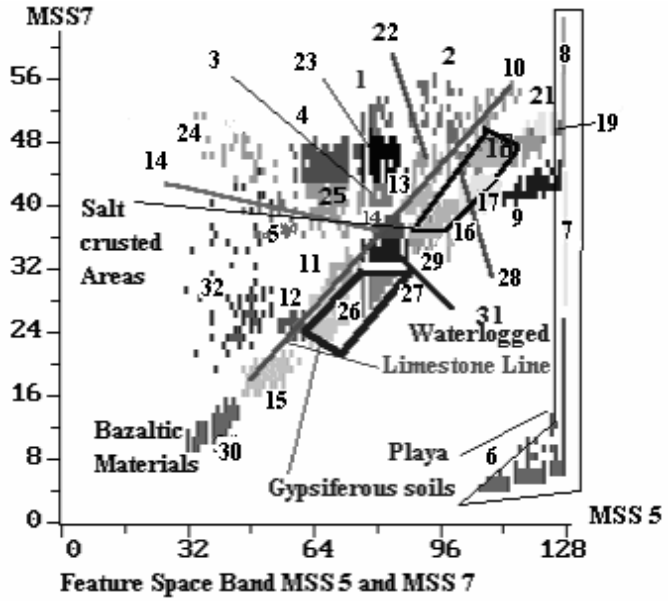

Figure 2. The feature space plot of MSS5-MSS7 that shows spectral signatures of 32 training areas (for the names and descriptions of training areas refer to the text and Table 1).

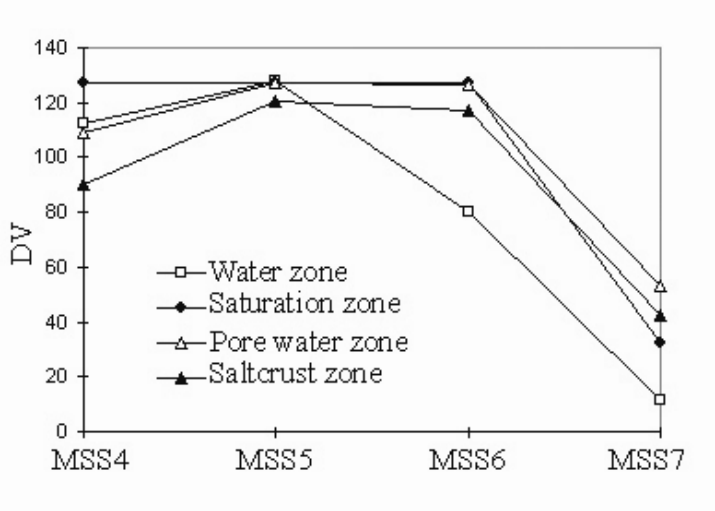

Figure 3. The spectral signatures of four zones of playa.

the playa and reported that the abundance of cations in the water zone is in the order:

$$Na^{+} > Mg^{++} > Ca^{++} > K^{+}$$

Their study indicated that chloride and bicarbonate are major anions but the concentration of chloride is more than bicarbonate. In the pore water zone the dominant anions are chloride and bicarbonate also and the abundance of cations is in the order:

$$Na^{+} > Ca^{++} > Mg^{++} > K^{+}$$

According to Braitsch (1962) among chloride salts the solubility constant of NaCl is very high while this value for $CaCl_2$ is very low and for $MgCl_2$ lies in between, consequently by increasing the concentration of soluble salts $CaCl_2$ subsides before $MgCl_2$ and NaCl. The dominant salts in the water zone of the playa are NaCl and $MgCl_2$ and in the pore water zone the dominant salts are NaCl and $CaCl_2$. Obviously, there is a rela-

[DOR: 20.1001.1.16807073.2009.11.1.2.1]

tionship between the position of the dominant salts and the geomorphologic zones of playas which are indicated on imagery data but more studies about these relations are required. Hunt (1966) studied the relationship of the position and the kind of salt in the playas of the Dead Sea. He found some annular rings of different salts both horizontally and vertically. While the centre of the playa was occupied by the chlorides, in the surrounding zones carbonates were dominant and the intermediate zones were covered by sulphates. Figures 2 and 3 show the spectral clusters of the playa have occupied a special part of the space. The salt crust zone of playa is spectrally different from other salt crusts which are developed in the alluvial plain and this could be due to the differences in mineral content or organic matter content.

The spectral signature of Bare soils I (which are plateaux with a dark desert varnish cover) was the same as of stable sand dunes or of Barchans so we could not discriminate these two landforms from each other spectrally. Ramesht (1992) and Givi (1994) considered the dominant wind direction of the area and expressed that the land covers of plateaux could be sources of materials for sand dunes in the west of Gavkhoni playa. As the clusters of the Grey limestone mountains and the Andesitic fans were coincided in all bands we merged them for classification.

Image Classification

After introducing the training pixels to the classifier, the separability of the training areas was examined by calculating means and standard deviations of classes, checking the clusters of the training areas in the feature space plots of images and finally by self-classification of training areas; if it was necessary the training areas were refined after each examination. The results of self-classification were examined in a contingence matrix and by considering the commission and omission pixels we refined the training pixels or merged the training areas with similar spectral signatures. For instance, spectral signatures of Bare soil I and Barchans or Andesitic fans and Grey limestone are identical so we merged them in two spectral classes. The accuracy of the final self-classification was 99.7%.

The Gaussian maximum likelihood classifier was used for image classification. A threshold of 5 percent was determined for the classifier which means a pixel will be classified if the probability of its membership for a certain spectral class is 95 percent or more otherwise the pixel will be indicated as unknown. The accuracy of the classified map was calculated in a contingency table (Table 4). We used 5,549 test and random pixels for evaluating the classified map. The test pixels had been selected during the fieldwork but they were not used for image classification and the random pixels were selected from available thematic maps like soil and geological maps**.** The results show that the overall accuracy of classification is 94.74 percent. Discrimination of Bare soil I from Barchans and Andesitic fans from Grey limestone was not possible spectrally but the location of Andesitic fans and Grey limestone mountains were geographically different so we delineated Andesitic fans visually after classification (Figure 4). For discrimination of the Bare soil I and Barchans classes the same approach was used.

The unclassified areas comprised 8% of the study area. By considering the definitions of all the spectral classes they were divided into thirteen physiographic units and a unit of water (Table 5).

The major physiographic units of the study area are mountains, piedmonts, sand dunes, valley and playa. The integration of spectral units forms components of physiographic units (Table 5). Relief type, subunits, faces, landforms and soils of mapping units were determined according to the field observations and available documents like soil maps or topographic maps (Table 6). Figure 4 shows the general physiographical units of the area. The scale of the map is not enough big to indicate the debris materials or separate colluviums from mountains.

[DOR: 20.1001.1.16807073.2009.11.1.2.1]

Table 4. Contingency table resulting from classifying test and random pixels.

			Number of pixels classified into category																														
Known category Type [a]	Number of pixels	Percentage correct	1	2	3	4	5	6	7	8	9	10	11	12	13	14	15	16	17	18	19	20	21	22	23	24	25	26	27	28	29	30	31	32
1	39	95.00	37																						2									
2	49	91.83	2	45																					2									
3	71	90.14	4		64																				3		3							
4	106	88.68				94	2																		4		5							
5	45	88.88					40																			2	1							2
6	201	100.00						201																										
7	123	92.68						9	114																									
8	94	94.43								85	9																							
9	63	96.82									61										1	1												
10	63	87.30										55																		8				
11	365	94.25											344															12	6				3	
12	267	91.75												256			11																	
13	342	87.54			2										305	15								8						12				
14	172	89.53			8										10	154																		
15	758	96.89													10		748																	
16	348	95.98																334	8					3							3			
17	150	94.00																9	141															
18	63	93.65																	14	59														
19	70	88.57																			62	6	2											
20	158	92.40																			5	146	7											
21	52	86.54																			2	5	45											
22	77	94.93																				1	1	75										
23	60	88.33	2		2	3																			53									
24	39	92.31				2	1																			36								
25	63	88.88			2	3	2																				56							
26	344	95.93																										330	14					
27	85	95.34																										3	82					
28	447	97.99										9																		438				
29	464	95.68													2			8	10												444			
30	154	100.00																														154		
31	113	93.81																											7				106	
32	104	89.42		3			1				1		4		1												1							93
∑	5,549	Average=92.80	Overall classification performance= (total correct pixels/total pixels)*100=(5257/5549)*100= 94.74%																															

[a] For descriptions of categories refer to table 1.

Table 5. Association of spectral classes of the classified MSS image and formation of physiographic units.

Informational unit	Spectral classes
1. Limestone Mountains	15. Grey limestone, 10. Limestone I, 11. Limestone II, 12. Limestone III, 13. Limestone IV, 14. Limestone V
2. Basaltic Mountains	30. Basaltic Mountain
3. Plateaue	26. Bare soils I, 27. Bare Soils II, 28. Saline Gypsiferous lands (Qom Formation)
4. Andesitic Fans	34. Andesitic fans
5. Alluvial Plain	Low salt affected vegetation I-II (classes 23 and 24), 25. Non to low salt affected vegetation, Moderately salt affected vegetation I-V (classes 1, 2, 3, 4 and 5), Fallow I-III (classes 20, 21 and 22),
6. Barchans	33. Stable sand dunes (Barchans)
7. Deflated Sands	29. Deflated sands
8. Water zone of playa	6. Water zone of playa
9. Saturation zone of playa	7. Saturation zone of playa
10. Pore water zone of playa	8. Pore water zone of playa
11. Salt crust zone of playa	9. Salt crust zone of playa
12. Salt crusted area	Salt crust I-IV (classes 16, 17, 18, 19)
13. Waterlogged areas	31. Waterlogged areas
14. Water	32. River, irrigation canals and flooded lands)

Table 6 . Characteristics of the physiographic units of the South East of Esfahan.

Mapping Unit	Relief Type	Subunit	Faces	Landform	Soils
Mountain	Steep slope High altitude	1. Limestone 2. Basaltic	Limestone and volcanic	Stony outcrop	No
Piedmont	Fans	4. Andesitic fans	Alluviums	Gravel, pebble with rills and gullies	No
	Plateaus	3. Plateaus - Saline-Gypsiferous plateaus	Alluviums	desert varnish cover gravel and conglomerate	Typic Gypsiorthids
		-Bare and Marl plateaus (Qom formation)	Evaporates	Saline marl deposits with salt crust	No
Sand dune	Deflated sands	7. Deflated sands	Active wind deposits,	Deflation, hollow sand	Buried soils sometimes Psamments
	Fixed sands	6. Barchans	fixed wind deposits	Barchans	
Valley	Alluvial plain and river plain	5. Alluvial Plain	Alluviums	Alluvial plain with silty clay loam, clayey texture and cropland	Typic Camborthids Typic Calciorthids
		12. Salt crusted areas	Evaporates	salt crust	Typic Salorthids
	Depressions (small)	13.Waterlogged areas	Evaporates and marshlands	Salt crust or marshland (depends on the season)	Typic Natrargids
Playa	Depression (large)	8. Water zone	Saline water		No
		9. Saturation zone	Wetland		
		10. Pore water zone	Evaporates		
		11. Salt crust zone	Evaporates		
Water		14. River and canals			

[DOR: 20.1001.1.16807073.2009.11.1.2.1]

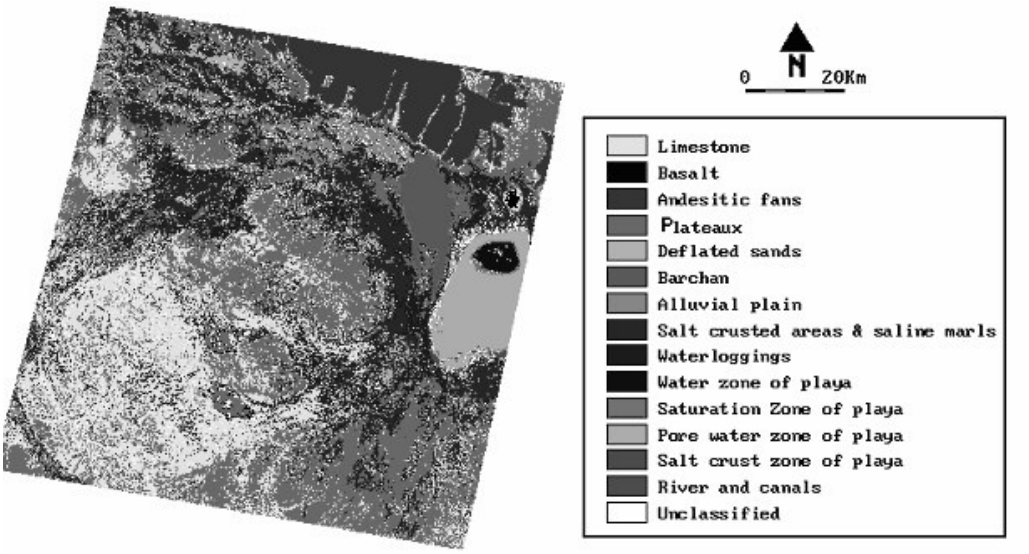

Figure 4. The physiographical map of the southeast of Esfahan.

CONCLUSION

The high sensitivity of Landsat MSS data and exposure of lands in arid zones provides sufficient facilities for detection of land covers in such areas. The weathering stage of materials, mineralogy and drainage condition of soils are all major indicators for differentiation of lands in arid areas. The results of this work demonstrate the high potential of Landsat MSS data for the differentiation of alluvial plains and classification of physiographic units. Different zones of the Gavkhoni playa like the water zone, saturation zone, pore water zone and salt crust zone were differentiated efficiently. The clusters of these zones occupy a specific space in the feature space of bands MSS5 and MSS7. The spectral signature of such units could be applied for mapping similar landscapes in arid zones. Further studies are required for identifying the minerals of these zones.

The sensors have the potential to differentiate the brackish water of the playa from the fresh water of Zayanderood River. It appears that the sensors are more sensitive to the mineralogy of land covers than to the surface texture of units; for instance, the texture of Barchans (stable sand dunes) and deflated sands are the same but the sensors differentiated them efficiently while the sensors were unable to differentiate Barchans from Bare soil I which is covered by desert varnish. The sensors were not able to differentiate Grey limestone from Andesitic fans, so using other ancillary data like the digital elevation model (DEM) of the area and its derivates may aid in increasing the efficiency of classification. There are several spectral classes for salt crusted areas and different factors like organic matter content, moisture content and mineralogy of salts which may lead to such variations. The results indicate that Landsat MSS data could be applied for the recognition of soils which are suffering from a shallow ground water table or are waterlogged. The authors recommend mineralogical analysis of sand dunes (Barchans) and the desert varnished covers of plateaues (Bare soil I) for determining the sources of different sand dunes.

[DOR: 20.1001.1.16807073.2009.11.1.2.1]

REFERENCES

1. Alizadeh, A. 1990. *Principles of Applied Hydrology*. Bonyade Farhangie Astane Ghodse Razavi Publisher), 519PP. (In Persian).
2. Academia Sinica Institute. 1987. *Data Compilation of Chinese Earth Resources Spectral Information*. 1055PP.
3. Baumgardener, M. F., Silva, L. F., Biehl, L. L. and Stoner, E. R. 1985. Reflectance Properties of Soils. *Adv. Agron*., **38**: 1-44.
4. Braitsch, O. 1962. *Entstehung und Stoffbestand der Salzlagerstatten. Mineralogie und Petrographie in Einzeldarstellungen. III.* Berlin.
5. Burrough, P. A., Van Gaans, P. F. M. and Macmillan, R. A. 2000. High-resolution landform Classification Using Fuzzy K-means. *Fuzzy Sets. Syst*., **113**: 37-52.
6. Chavez, P. S. Jr., Guptill, C. and Bowell, J. A. 1984. Image Processing Techniques for Thematic Mapper Data. *Am. Soc. Photogram. Remote Sens.*, PP. 728-752.
7. Chavez, P. S., Berlin, G. L. and Sowers, L. B. 1982. Statistical Method for Selecting Landsat MSS Ratios. *J. Appl. Photographic Eng*., **8**: 23-30.
8. Donoghue, D. N., Reid Thomas, D. C. and Zong, Y. 1994. Mapping and Monitoring the Intertidal Zone of the East Coast Using Remote Sensing Techniques and a Coastal Monitoring GIS. *MarinE Technol. Soc*., **28**: 19-29.
9. Everitt, J. H., Escobar, D. E., Gerbermann, A. H. and Alaniz, M. A. 1988. Detecting Saline Soils with Video Imagery. *Photogramm. Eng. Remote Sens*., **54**: 1283-1287.
10. Ganji, M. H. 1960. *Iranian Rainfall Data.* Tehran, Univ. of Tehran, Arid Zone Research Centre.
11. Givi, J. 1994. Genesis and Characteristics of Representative Alluvial Soils from Different Climatic Zones in Iran. Ph. D. Thesis, University of Ghent, Faculty of Science, 407 PP.
12. Greenbaum, D. 1987. Lithological Discrimination in the Central Snowdonia Using Airborn Mmultispectral Scanner Imagery. *Int. J. Remote Sens*., **8(6)**: 799-816.
13. Hengl, T. and Rossiter, D. G. 2003. Supervised Landform Classification to Enhanced and Replace Photo-interpretation in Semi-detailed Soil Survey. *Soil Sci. Soc. Am. J*., **67**: 1810-1822.
14. Hunt, C. B., Robinson, T. W., Bowles, W. A. and Washburn, A. I. 1966. *Hydrologic Basin, Death Valley*, California, US Geological Survey, Professional Paper 494B.
15. ITC, 2001. *ILWIS 3.0 Academic User's Manual*. ITC, Enschede, The Netherlands.
16. Krinsley**,** D. B. 1970. *A Geomorphologic and Paleoclimatological Study of Playas of Iran*. US Geology Survey, Final Scientific Report, Air Force Cambridge Research Laboratories Hanscom Field, Bedford, Massachusetts, Parts I and II, 488PP.
17. Leblance, M. J., Leduc, C., Stagnitti, F., Van Oevelen, P. J., Jones, C., Mofor, L. A., Razack, M. and Favreau, G. 2006. Evidence for Megalake Chad, North-central Africa, During the Late Quaternary from Satellite Data. *Paleogeomorphol. Paleoclimatol.*, **230**: 230-242.
18. Lane, S. N., Richards, K. S. and Chandler, J. H. 1998. *Landform Monitoring, Modeling and Analysis*. Wiley, J. and Sons, New York.
19. Lillesands T. M. and Kiefer, R. W. 2004. *Remote Sensing and Image Interpretation*. 4th Ed. Wiley New York, P. 725.
20. Mather, P. M. 1999. *Computer Processing of Remotely-Sensed Images*. Wiley, J. and Sons, Chichester, New York, Weinheim, Brisbane, Singapore, Torento.
21. McManus, J., Duck, R. W. and Anderson, J. M. 1999. The Relative Merits and Limitation of Thermal Radiometric Measurements in Estuarine Studies. *Int. J. Remote Sens*., **20**: 549-559.
22. Milton, E. J., Gilvear, D. J. and Hooper, I. D. 1995. Investigation Change in Fluvial Systems Using Remotely Sensed Data. In: "*Changing River Channels*", Grunell, A. and Petts, G. (Eds.), Wielly, J. and Sons. Chichester, PP. 276-301.
23. Muller, E., Decamps, H. and Dobson, M. K. 1993. Contribution of Space Remote Sensing to River Studies. *Fresh Water Biol*., **29**: 301-312.
24. Odeh, I. O. A., McBratney, A. B. and Chittleborough, D. J. 1994. Spatial Prediction of Soil Properties from Landform Attributes Derived from Digital Elevation Model. *Geoderma.,* **63**: 197-214.

[DOR: 20.1001.1.16807073.2009.11.1.2.1]

25. Rainey, M. P., Tyler, A. N., Gilvear, D. J., Bryant, R. G. and McDonald, P. 2003. Mapping Intertidal Estuarine Sediment Grain Size Distributions through Airborne Remote Sensing. *Remote Sens. Environ.*, **86**: 480-490.
26. Ramesht, H. 1992. The Zayanderud River Terraces and Their Influence on Geomorphology of Esfahan Territory (In Persian), Ph. D. Thesis, Esfahan University, Iran.
27. Rencz, A. N. 1999. *Remote Sensing for Earth Sciences. Manual of Remote Sensing*, 3rd Ed. Volume 3. Published in Cooperation with American Society for Photogrametry and Remote Sensing. 707PP.
28. Richards, J. A. 1986. *Remote Sensing Digital Image Analysis an Introduction*. Springer-Verlag Berlin Heidelberg, New York, London, Paris, Tokyo, 281PP.
29. Richardsons, A. J. and Wiegand, A. L. 1977. Distinguishing Vegetation from Soil Background Information. *Photogramm. Engin. Remote Sens*., **43 (12)**: 1541-1552.
30. Schmidt, J., Hennrich, K. and Dikau, R. 1998. Scales and Similarities in Runoff Processes with Respect to Geomorphology. Proc. 3rd International Conference on GeoComputation, University of Bristol, UK.
31. Shaw, P. A., Thomas, G. and David S. 1997. Playas, Pans and Salt Lakes. In: "*Arid Zone Geomorphology, Process, form and Change Indrylands*". David, S. and Thomas, G. (Eds.), University of Sheffield, Wiley, J. and Sons Ltd., 713PP.
32. Swain, P. H. and Davis, M. S. 1978. *Remote Sensing: The Quantitative Approach*, N. Y. McGraw-Hill.
33. Webster R. and Oliver, M. L. 1990. *Statistical Methods in Soil and Land Resource Survey*. Oxford Univ. Press, Oxford, 316 PP.
34. Zahedi, M. 1976. *Explanatory Text of the Esfahan Quadrangle Map* (1: 250,000), No. F8, Geological Survey of Iran, Ministry of Industry and Mines, Tehran.
35. Zink, J. A. 1988. *Physiography and Soils. ITC Lecture Notes,* Enschede, The Netherlands.
36. Zink, J. A. and Valenzuela, C. R. 1990. Soil Geographic Database: Structure and Application Examples. *ITC J.*, **990**: 270-294.

ارزیابی قابلیت اطلاعات Landsat MSS برای تهیه نقشه فرم اراضی در مناطق خشک
مطالعه موردی در مرکز ایران

م. نادری خراسگانی و م. دی داپر

چکیده

این تحقیق برای ارزیابی پتانسیل اطلاعات Landsat MSS برای تهیه نقشه فرم اراضی (Landform) در جنوب شرقی اصفهان مورد استفاده قرار گرفت. با استفاده از نقشه‌ها و گزارشهای مربوط به منطقه که با کار میدانی پشتیبانی می‌شدند بانک اطلاعات منطقه تشکیل شد. با به‌کارگیری سی و دو محل آموزشی (Training areas) روش طبقه‌بندی نظارت شده (Supervised classification) مورد استفاده قرار گرفت. مجزا بودن کلاسهای طیفی در فضای دو بعدی عوارض (Feature space) و خود طبقه‌بندی (Self-classification) آزمون گردید. صحت طبقه‌بندی به کمک پیکسلهای آزمایشی و تصادفی تعیین گردید. نتایج نشان‌دهنده پتانسیل اطلاعات ماهواره‌ای برای تعیین فرم اراضی و بخشهای مختلف پلایا می‌باشد. نهشته‌های شنی (شنهای مواج و برخانها) انعکاسهای متفاوتی را نشان می‌دهند که می‌تواند ناشی از کانیهای

تشکیل دهنده آنها باشد. دسته پیکسلهای مربوط به خاکهای شوری و رطوبتهای مختلف بر روی خط خاک (Soil line) و سنگ آهکهای موجود در منطقه در کنار خط خاک قرار می‌گیرند. اطلاعات لندست MSS قادر به جداسازی برخانها از بعضی اراضی بایر و مخروط افکنه‌های آندزیتی از سنگ آهک نیستند. فرمهای اراضی اصلی منطقه شامل کوهها، دشت‌سر(Piedmont)، تپه‌های شنی، دشتها و پلایا می‌باشد. نتایج همچنین نشان می‌دهد که تلفیق مشاهدات میدانی و طبقه‌بندی نظارت شده می‌تواند نبود نقشه‌های توپوگرافی را برای بعضی مناطق جبران کند و امضای طیفی (Spectral signature) عوارض زمینی می‌تواند برای تمایز فرمهای مختلف اراضی مورد استفاده قرار گیرد.

[DOR: 20.1001.1.16807073.2009.11.1.2.1]